Isocyanide substituent influences reductive elimination versus migratory insertion in reaction with an $[Fe_2(\mu\text{-}H)_2]^{2+}$ complex

*Titto Sunil John[a], Łukasz Dobrzycki[b], Vincent J. Catalano[c], and Leslie J. Murray[a,]**

[a] Center for Catalysis and Florida Center for Heterocyclic Chemistry, Department of Chemistry, University of Florida, Gainesville, FL, 32611, U.S.A.

[b] Department of Chemistry, University of Florida, Gainesville, FL, 32611, U.S.A.

[c]. Department of Chemistry, University of Nevada, Reno, NV, 89557, U.S.A.

*Correspondence: murray@chem.ufl.edu

KEYWORDS: Isocyanide, iron-hydride, migratory insertion, reductive elimination, aldimine, iminoformyl

Abstract

Iron hydrides are proposed reactive intermediates for N_2 and CO conversion in industrial and biological processes. Here, we report a reactivity study of a low-coordinate di(μ-hydrido)diiron(II) complex, $Fe_2(\mu\text{-}H)_2\mathbf{L}$, where $\mathbf{L}^{2-}$ is a bis(β-diketiminate) cyclophane, with isocyanides, which have related electronic structures to N_2 and CO. The reaction outcome is influenced by the isocyanide

substituent, with 2,6-xylyl isocyanide leading to H_2 loss, to form a bis(μ-1,1-isocyanide)diiron(I) complex, whereas all the other tested isocyanides insert into the Fe–H bond to give (μ-1,2-iminoformyl) complexes. Steric bulk of the isocyanide substituent determines the extent of insertion (*i.e.*, into one or both Fe–H–Fe units) with *tert*-butyl isocyanide reacting to yield the mono-(μ-1,2-iminoformyl)diiron(II) complex, exclusively, and isopropyl- and methyl-isocyanides affording the bis-(μ-1,2-iminoformyl)diiron(II) products. Treatment of Fe_2(μ-1,2-CHNtBu)(μ-H)**L** with 2,6-xylyl isocyanide (or XylNC) yields Fe_2(μ-XylNC)$_2$**L** and yields the aldimine, $tBuNCH_2$ as one of the organic products.

Introduction

Activation of dinitrogen and carbon monoxide remain active areas of chemical research, given relevance to biological and industrial N_2 fixation and the Fischer-Tropsch process, respectively. Metal hydrides are proposed as reactive intermediates in these processes, with particular interest in the reactivity of iron hydrides insofar as this metal is common to catalysts for both N_2 and CO activation. For example, proposed dissociative adsorption of H_2 and either N_2 or CO on catalyst surfaces for the Haber-Bosch or Fischer-Tropsch processes, respectively, lead to NH_3 or hydrocarbon formation.[1–3] In homogeneous systems, metal hydrides serve as a type of protecting group for low-valent metal centers as H_2 reductive elimination unmasks the reduced metal centers.[4–8] Isocyanides are a useful proxy for CO and N_2 for reactivity studies; these three molecules have a pair of accessible π-accepting orbitals, albeit with differences in the σ donor strength and π-acidity.[9] Unsurprisingly then, isocyanides are competent inhibitors or alternative substrates for N_2 in the catalytic systems noted above.[4,10,11] In contrast to N_2, the steric bulk of the isocyanide substituent provides an additional handle to limit the metal coordination number, and stabilize structural analogs of proposed reactive intermediates otherwise inaccessible using CO or

N_2.[12–15] Typically, isocyanides react with metal hydrides by migratory insertion into the M–H bond to yield iminoformyl (–C(H)NR) or aminocarbyne (–CN(H)R) complexes or by H_2 reductive elimination followed by isocyanide coordination in terminal or μ-1,1 modes depending on complex nuclearity.[16–20] Notably, Rosenberg and coworkers observed differences in the site of migratory insertion (*viz.* C or N) in the reaction of a triosmium dihydride cluster with isocyanides as a function of the isocyanide substituent,[21] and similar results were reported for $W_2(\mu\text{-H})_2(CO)_4(\eta^5\text{-Cp})_2$.[22] Comparable control of insertion vs. reductive elimination can be afforded by tuning the steric demands of the ancillary ligands in the dimanganese di(μ-hydride) complexes.[21] (Scheme 1).

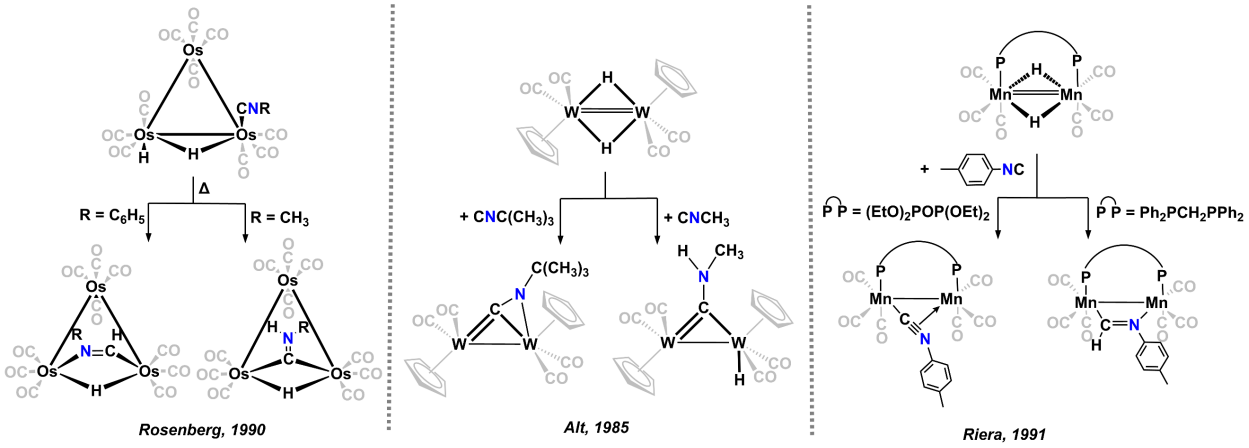

Scheme 1. Prior reports of reactivity of polynuclear transition metal hydrides with isocyanides demonstrating dependence on isocyanide substitiuent or ancillary ligand.

Previously, our group reported that a di(μ-hydrido)diiron complex, $Fe_2(\mu\text{-H})_2\mathbf{L}$ ($\mathbf{L}^{2-}$ = bis(β-diketiminate)cyclophane) reacts with CO to reductively eliminate H_2 and yield a di(μ-carbonyl)diiron(II) complex, $Fe_2(\mu\text{-CO})_2\mathbf{L}$ (Scheme 2).[24] Here, we extend that work towards reaction with isocyanides and observe a substituent-dependent reductive elimination of H_2 or migratory insertion. Varying the equivalents of isocyanide used or the substituent from methyl to *tert*-butyl results in retention of one μ-hydride ligand to yield the (μ-hydrido)(μ-κC:κN-iminoformyl) diiron product instead of the bis(iminoformyl) diiron(II) complex observed for

reaction with 2 equiv. of methyl and isopropyl isocyanides. Reaction of $Fe_2(\mu\text{-HCNtBu})(\mu\text{-H})\mathbf{L}$ with xylyl isocyanide effects aldimine loss, and is a rare example of isocyanide to aldimine conversion.[12] The substituent controls over the extent of insertion as well as over reductive elimination, which is observed here is distinct from precedent.

Experimental Methods

General Considerations. All manipulations were performed within an Ar-filled Vigor glovebox unless otherwise stated. Tetrahydrofuran (THF), benzene, toluene, *n*-hexane, and diethyl ether were purchased from Sigma-Aldrich, dried using an Innovative Technologies solvent purification system (now Inert, Amesbury, MA, USA), transferred to the glovebox, and stored over activated 3 Å molecular sieves (200 °C, < 20 mT) for at least 24 h prior to use, with water contents below

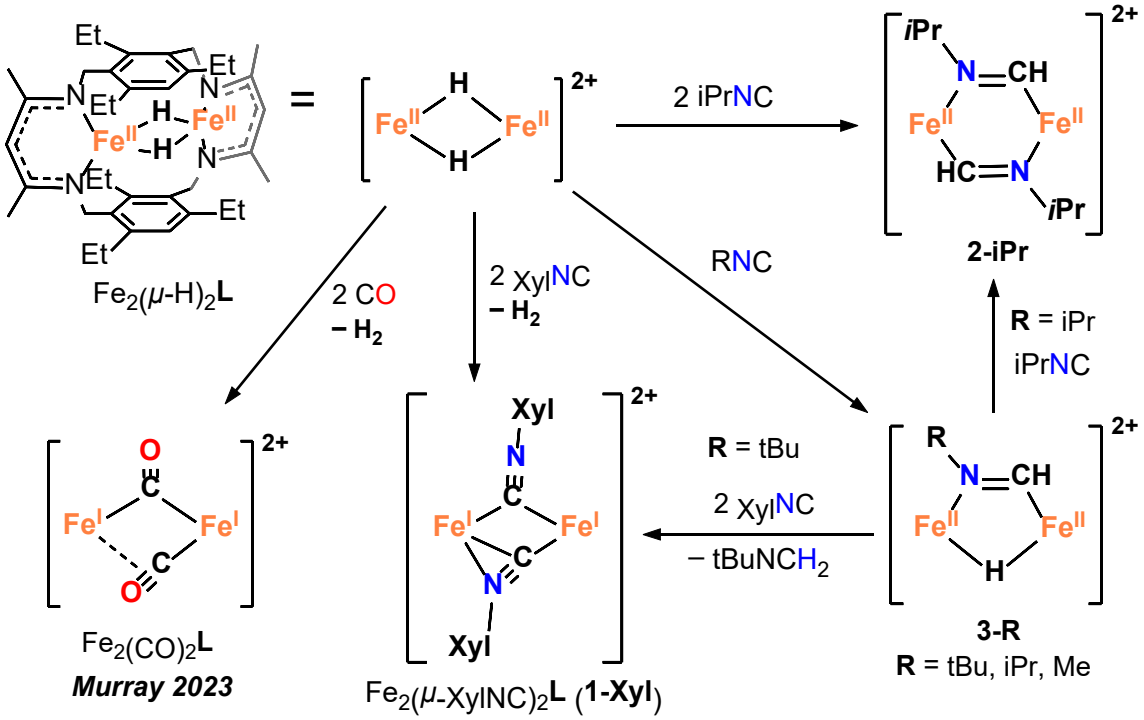

Scheme 2. Synthesis of the reported complexes from $Fe_2(\mu\text{-H})_2\mathbf{L}$ by treatment with isocyanides. Complexes are abbreviated as the diiron core with $\mathbf{L}^{2-}$ omitted for clarity.

25 ppm determined using a Mettler Toledo C20 Coulometric Karl-Fischer titrator. C_6D_6 was purchased from Cambridge Isotope Laboratories, dried at reflux over CaH_2, then distilled, degassed, transferred to the glovebox, and stored over activated 3 Å molecular sieves. 2,6-dimethylphenyl-, phenyl-, *tert*-butyl- and isopropyl- isocyanides were purchased from Oakwood Chemical (Estill, SC, USA). Methyl isocyanide and $Fe_2(\mu\text{-}H)_2$**L** were prepared as reported elsewhere.[24,25] ^{1}H Nuclear Magnetic Resonance (^{1}H NMR) spectra were recorded on a Bruker 400 MHz spectrometer or an Inova 500 MHz equipped with a three-channel indirect detection probe with *z*-axis gradients. ^{1}H NMR spectra of paramagnetic complexes were collected with a 0 s relaxation delay, an acquisition time of 0.3 s, and for 256 scans. ^{1}H NMR spectra of organic diamagnetic products were collected using a 1.0 s relaxation delay, a 3.6 s acquisition time, and averaged over 16 scans. Chemical shifts were reported in δ (ppm) and were referenced to residual internal C_6D_5H resonance at δ_H = 7.16 ppm for benzene-d_6. FT-IR spectra were collected on drop-cast samples using a ThermoFisher Scientific Nicolet iS5 spectrometer with an iD7 ATR stage operated by the OMNIC software package with a 1.0 cm^{-1} resolution and 32 scans per sample. Mass spectrometry data were collected on an Agilent 6230 ESI-TOF for which the flow lines were extensively rinsed with anhydrous air-free THF prior to use, in positive mode by direct injection of samples as anhydrous THF solutions, and with a gas temperature and a fragmentation voltage of 350 °C and 125.0 V, respectively.

X-ray Crystallography. Low-temperature X-ray diffraction data for **1-Xyl**, **2-iPr,** and **3-tBu** were collected on a Rigaku XtaLAB Synergy diffractometer coupled to a Rigaku Hypix detector using CuKα radiation (λ = 1.54184 Å) from a PhotonJet micro-focus X-ray source at 100 K. The diffraction images were processed and scaled using the CrysAlisPro software.[26] The structures were solved through intrinsic phasing using SHELXT and refined against F^2 on all data by full-

matrix least squares with SHELXL following established refinement strategies.[27–29] All non-hydrogen atoms were refined anisotropically. All hydrogen atoms bound to carbon were included in the model at geometrically calculated positions and refined using a riding model. The isotropic displacement parameters of all hydrogen atoms were fixed to 1.2 times the U_{eq} value of the atoms they are linked to (1.5 times for methyl groups). In the structure of **3-tBu,** the *t*-butyl group and one ethyl group of the arene cap in $\mathbf{L^{2-}}$ ancillary ligand are disordered over two sites with refined occupancy yielding 0.587(5):0.413(5) and 0.55(3):0.45(3) respectively (Figure S26). To preserve reasonable geometry of disordered fragments, various distance and angle restraints were used. Details of the data quality and a summary of the residual values of the refinements are listed in Tables S2, S3, and S5 for **1-Xyl**, **2-iPr** and **3-tBu**, respectively.

The X-ray measurement of **3-iPr** and **3-Me** were performed at 100(1) K and 180(1) K respectively on a BRUKER D8 Venture with PHOTON III four-circle diffractometer system equipped with a INCOATEC IμS 3.0 micro-focus X-ray tube (MoKα, λ = 0.71073 Å) and a HELIOS multilayer optics monochromator. Frames were collected with Bruker APEX3 program. [30] The frames were integrated with the Bruker SAINT software package using a narrow-frame algorithm.[31] Data were corrected for absorption effects using the Multi-Scan method (SADABS).[32] The structure of **3-iPr** was solved through the intrinsic phasing method and refined using the Bruker SHELXTL software package.[28,33] The structure is disordered with part of the molecule including phenyl moiety with substituents distributed over two positions with a refined occupancy ratio yielding 0.565(6):0.435(6) (Figure S26). A number of distance and angle restraints were used to preserve reasonable geometry of disordered fragment. All non-hydrogen atoms (including disordered groups) were refined anisotropically with applied restraints for modelling ADPs of some disordered atoms. All hydrogen atoms, except the hydride ligand, were placed in calculated

positions and refined within the riding model. Coordinates and temperature factor of the hydride ligand are fully refined. Temperature factors of all C-bound H atoms were not refined and were set to be either 1.2 or 1.5 times larger than U_{eq} of the corresponding heavy atom. Details of the data quality and a summary of the residual values of the refinements are listed in Tables S4. The structure of **3-Me** was solved through direct method using the Bruker SHELXTL software package.[28,33] The structure is disordered with part of the molecule, including one Fe site, one phenyl moiety with substituents and the coordinated imine, distributed over two positions with refined occupancy ratio of 0.576(14):0.424(14) (Figure S26). As for prior structure solutions, distance and angle restraints were employed to preserve a reasonable geometry of the disordered fragment. All non-hydrogen atoms (including disordered groups) were refined anisotropically with applied restraints for modelling ADPs of some disordered atoms. All hydrogen atoms, except for the hydride, were placed in calculated positions and refined within the riding model. The hydride ligand coordinated to the Fe centers is disordered over three positions and located between the heavy atoms. Coordinates of the disordered hydride ligands are refined with Fe-H distance restraints. Temperature factors of all H atoms were not refined and were set to be either 1.2 or 1.5 times larger than U_{eq} of the corresponding heavy atom. Details of the data quality and a summary of the residual values of the refinements are listed in Table S6.

$Fe_2(\mu$-XylNC)$_2$L, 1-Xyl. To a solution of $Fe_2(\mu$-H)$_2$**L** (50.0 mg in PhMe, 73.4 μmol) stirred with a Pyrex-coated magnetic stir bar 2,6-xylyl isocyanide (20.2 mg in 2 mL PhMe, 154 μmol) was added dropwise. The reaction was stirred at ambient temperature for 3 h over which the reaction mixture gradually changed from dark brown to reddish-brown. The solvent was removed under reduced pressure to afford **1-Xyl** as a dark red solid (57.6 mg, 83.4%). Single crystals suitable for X-ray diffraction were grown by cooling a saturated solution of as-isolated **1-Xyl** in PhMe to -

33°C for 2 d to afford dark brown crystals (8.0 mg, 12.6%). The solution was saturated at 60 °C and filtered through a Celite plug, which was pre-rinsed with anhydrous PhMe. ^{1}H NMR (400 MHz, C_6D_6, 298 K) δ (ppm): 101.47, 24.43, 6.96-7.39, 2.11, 2.01, 0.27, -40.20, -45.16, -80.54, and -90.41. ATR-IR (cm^{-1}): 2960, 2925, 2867, 1854, 1820, 1605, 1563, 1525, 1460, 1428, 1399, 1372, 1328, 1012, 763. Anal. Calc. for $C_{56}H_{72}N_6Fe_2 \cdot 0.4$ THF (%): C 71.49, H 7.71, N 8.93. Found: C 70.97, H 7.90, N 8.49. μ_{eff} = 6.9(2) μ_B

Fe$_2$(μ-κ*C*:κ*N*-HCNiPr)$_2$L, 2-iPr. Fe$_2$(μ-H)$_2$**L** (50.0 mg, 73.4 μmol) was dissolved in 4 mL PhMe taken in a 20 mL scintillation vial. The sample was stirred using a PTFE stir bar and cooled to -33 °C. To this sample, 1.5420 mL of a 0.1 M stock solution of iPrNC in PhMe precooled to -33 °C was added dropwise. The resulting dark red solution was stirred for 12 h at ambient temperature. Volatiles were removed under reduced pressure to yield **2-iPr** as a dark brown solid (49.6 mg, 83.1%). Single crystals suitable for X-ray diffraction analysis were grown by layering hexanes on a saturated PhMe solution of **2-iPr** at -33 °C for 2 d (8.0 mg, 13.3%). The PhMe solution was saturated by heating to 60 °C briefly (< 30 s) and then filtered through a Celite plug, which was pre-rinsed with anhydrous PhMe. ^{1}H NMR (400 MHz, C_6D_6, 298 K) δ (ppm): 82.94, 70.54, 58.19, 54.54, 4.22, 2.12, 0.83, 0.31, 0.30, -2.22, -9.61, -20.74, -22.18, -26.15, -28.15. ATR-IR (cm^{-1}): 2960, 2925, 2868, 1515, 1466, 1429, 1397, 1372, 1325, 1016 Anal. Calc. For $C_{46}H_{70}N_6Fe_2$ (%): C 67.47, H 8.62, N 10.26. Found: C 67.20, H 8.23, N 9.16. μ_{eff} = 5.7(2) μ_B

Fe$_2$(μ-κ*C*:κ*N*-HCNiPr)(μ-H)L, 3-iPr. Fe$_2$(μ-H)$_2$**L** (10.0 mg, 14.6 μmol) was added to a 20 mL scintillation vial containing a Teflon magnetic stir bar and 4.0 mL PhMe, and the solution cooled to -33 °C. To this solution, iPrNC in PhMe (147.0 μL, 0.1 M solution, 14.7 μmol) cooled to -33 °C was added dropwise and stirred at ambient temperature for 12 h. The solvent was then removed under reduced pressure to afford a brownish-red solid (10.1 mg, 91.0 %). Single crystals suitable

for X-ray diffraction were obtained by the dissolution of the brownish-red solid in benzene (70 °C), followed by the slow evaporation of the solvent into mineral oil at ambient temperature after 7 d. ^{1}H NMR (400 MHz, C_6D_6, 298 K): δ (ppm): 104.39, 101.11, 93.29, 84.14, 78.12, 9.31, 5.41, 1.38, 1.26, -3.51, -5.29, -16.79, -33.17, -35.13, -39.40, -47.84. ATR-IR (cm^{-1}): 2961, 2924, 2868, 1520, 1457, 1430, 1394, 1372, 1322, 1249, 1014. Anal. Calc. for $C_{42}H_{63}N_5Fe_2$ (%): C 67.29, H 8.47, N 9.34. Found: C 66.89, H 8.57, N 9.02. μ_{eff} = 5.4(2) μ_B

Fe$_2$(*μ*-κ*C*:κ*N*-HCN*t*Bu)(*μ*-H)L, 3-tBu. To a 20 mL scintillation vial charged with Fe$_2$(*μ*-H)$_2$**L** (150.0 mg, 220.0 μmol), 4.0 mL PhMe, and a PTFE magnetic stir bar at ambient temperature, tBuNC (27.5 mg, 330.0 μmol) dissolved in 2.0 mL PhMe was added dropwise. The reaction mixture was stirred at ambient temperature for 3 h after which the solvent was evaporated under reduced pressure affording **3-tBu** as a dark red solid (134.7 mg, 80.2%). Single crystals for XRD diffraction were obtained as described for **2-iPr** (13.9 mg, 8.2%). ^{1}H NMR (400 MHz, C_6D_6, 298 K): δ (ppm): 94.17, 87.58, 74.81, 65.20, 9.56, 8.86, 4.64, 0.87, -2.77, -15.48, -27.86, -30.60. ATR-IR (cm^{-1}): 2961, 2924, 2868, 1520, 1457, 1430, 1394, 1372, 1322, 1249, 1014. Anal. Calc. for $C_{43}H_{65}N_5Fe_2$ (%): C 67.63, H 8.58, N 9.17. Found: C 67.38, H 8.69, N 9.05. μ_{eff} = 5.6(2) μ_B

Fe$_2$(*μ*-κ*C*:κ*N*-HCNMe)(*μ*-H)L, 3-Me. A 20 mL scintillation vial was charged with Fe$_2$(*μ*-H)$_2$**L** (5.0 mg, 7.3 μmol), 4 mL PhMe, and a Pyrex magnetic stir bar, and then cooled to -33 °C. To this solution, MeNC (36.7 μL, 0.1 M in PhMe, 3.7 μmol) pre-cooled to -33 °C was added dropwise. The reaction was stirred at -33 °C for 12 h, and then at ambient temperature for 30 min. The reaction was then cooled to -33 °C, followed by dropwise addition of a second portion of MeNC (36.7 μL, 0.1 M in PhMe, 3.7 μmol). As before, the reaction was stirred at -33 °C for 12 h, and then for 30 min at ambient temperature. *NOTE: Sequential addition of 0.5 equivalent of MeNC is*

required as addition of one equivalent affords a mixture of the 1 equiv. and 2 equiv. products, and unreacted $Fe_2(\mu\text{-}H)_2$***L***. All volatile species were removed under reduced pressure to yield a dark brown solid (4.9 mg, 6.8 μmol). Single crystals suitable for X-ray diffraction were obtained by slow evaporation from a saturated solution in diethyl ether at ambient temperature. ^{1}H NMR (400 MHz, C_6D_6, 298 K) δ (ppm): 96.25, 92.28, 90.40, 89.67, 81.62, 9.60, 2.11, 0.12, -3.17, -7.40, -16.55, -18.69, -34.54, -36.03. ATR-IR (cm^{-1}): 2959, 2927, 2869, 1527, 1459, 1428, 1398, 1372, 1329, 1019. Anal. Calc. for $C_{40}H_{59}N_5Fe_2 \cdot 1\ C_4H_{10}O$ (%): C 66.41, H 8.74, N 8.80. Found: C 66.05, H 8.48, N 9.17. μ_{eff} = 4.2(2) μ_B

Reaction of $Fe_2(\mu\text{-}H)_2$L with 2 equiv. MeNC. This reaction was performed as described for the 1 equiv. reaction above, except that MeNC was added in four separate portions (4 × 36.7 μL, 0.1 M in PhMe, 4 × 3.7 μmol). The dark, red-colored reaction mixture was then dried *in vacuo* to yield a dark brown solid (5.3 mg,7.0 μmol). ^{1}H NMR (400 MHz, C_6D_6, 298 K) δ (ppm): 121.23, 119.63, 94.62, 84.95, 62.24, 20.71, 0.77, -0.57, -3.91, -7.14, -39.92, -43.64, -48.95, -51.32, -79.76. ATR-IR (cm^{-1}):2958, 2923, 2867, 1512, 1459, 1427, 1394, 1371, 1319, 1015.

Reaction of $Fe_2(\mu\text{-}H)_2$L with 2 equiv. PhNC. $Fe_2(\mu\text{-}H)_2$**L** (53.7 mg, 78.9 μmol) was dissolved in 4.0 mL PhMe. To the scintillation vial containing this mixture, a solution of PhNC (2.1350 mL, 77.58 mM in PhMe, 165.7 μmol) was added dropwise resulting in a color change to reddish brown upon mixing. The reaction was stirred for 90 min at ambient temperature, and then dried under reduced pressure to yield a brown solid (66.1 mg). ^{1}H NMR (400 MHz, C_6D_6, 298 K) δ (ppm): 90.24, 83.84, 69.16, 65.07, 16.55, 9.51, 4.26, 2.09, 1.16, 0.44, -2.10, -7.28, -27.40, -30.80. ATR-IR (cm^{-1}): 2959, 2925, 2867, 1592, 1518, 1458, 1429, 1393, 1372, 1322, 1018.

Results and Discussion

Treating $Fe_2(\mu\text{-}H)_2$**L** with 2 equiv. of 2,6-xylyl isocyanide (XylNC) in toluene at ambient temperature afforded a C_{2v} symmetric species, **1-Xyl**, and H_2 (δ = 4.50 ppm), based on ^{1}H NMR spectra of product mixture (Figure S1, S4). IR spectra recorded on **1-Xyl** have strong absorptions at 1820 cm^{-1} and 1853 cm^{-1}, consistent with bound RNC ligands (Figure S3).[34] A transient species was observed by NMR spectroscopy 10 min after the addition of XylNC at ambient temperature (Figure S5). Resonances for this transient disappear as the reaction proceeds with those for **1-Xyl** concomitantly increasing in intensity, consistent with, but not confirmatory of, this transient as a reaction intermediate. Reaction of **1** with fewer equiv. of XylNC results in unreacted $Fe_2(\mu\text{-}H)_2$**L** and **1-Xyl**. The solid-state structure of **1-Xyl** contains a diiron core with one isocyanide bound in a μ-η^1:η^2 fashion and between the ligand arene rings, and a second isocyanide coordinated in a μ-1,1 mode (Figure 1). The observed solid state C_s symmetry of **1-Xyl** differs from the solution phase C_{2v} symmetry, implying that the isocyanide coordination modes are fluxional on the NMR timescale at ambient temperature or the observed asymmetry arises from crystal packing effects. The μ-η^1:η^2-xylylisocyanide N≡C bond length is longer as compared to that of the μ-1,1-isocyanide (*viz.* 1.275(1) Å vs. 1.189(1) Å, respectively), as expected given the greater extent of formal sp^2 hybridization based on the C≡N–C_{xylyl} bond angle (*viz.* 138.4(9)° vs. 158.6(1)°, respectively).[22,35] Typically, the μ-η^1:η^2 mode is observed for N_2 and isocyanides bound to reduced early transition metals and is rarely observed for late 3*d* metals, including the few examples of heterometallic dinuclear complexes of Fe and a 4*d* transition metal.[36–55] The only structurally characterized examples of a μ-η^1:η^2-isocyanide in a homometallic dinuclear 3*d* metal complex are the dimanganese(0) and dititanium(III) complexes reported by Balch and Cloke, respectively.[56,57] A holistic comparison of the reported N≡C, M–η^2:C, and M–η^2:N bond distances and the assigned ν_{NC} energies and those for **1-Xyl** highlight that the bond metrics are poorly correlated with the IR

data (Table S1). For example, the N≡C bond distance in $Mn_2(\mu\text{-}\eta^1\text{:}\eta^2\text{-}p\text{-}CH_3C_6H_4NC)(Ph_2PCH_2PPh_2)_2(CO)_4$ of 1.2479(2) Å is comparable to that in **1-Xyl**, yet the ν_{NC} is observed at 1661 cm^{-1} vs. 1820 cm^{-1} for **1-Xyl**.[56,57] Nonetheless, the trend that **1-Xyl** exhibits less activation of the isocyanide agrees with the greater electronegativity of Fe vs. metals in other reported examples and is consistent with IR data for a heterometallic dinuclear complex containing an η^2-isocyanide bound to an Fe center.[38] In contrast to the local pseudo-tetrahedral geometry (τ_4 = 0.72 and 0.85) at each iron center of **1-Xyl**, a previously reported mononuclear bis(isocyanide) Fe(I) β-diketiminate complex exhibits square planar geometry, likely a consequence of the

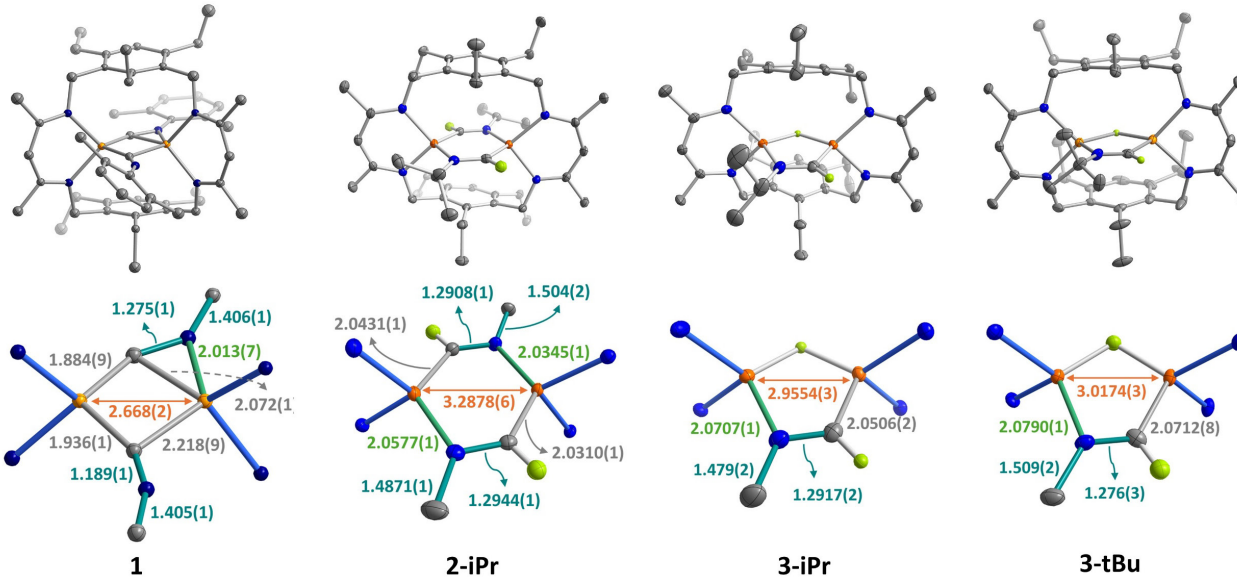

Figure 1. Crystal structures of **1-Xyl, 2-iPr, 3-iPr** and **3-tBu** with thermal ellipsoids at 50% probability level from left to right, respectively (top). Solvent molecules and hydrogen atoms removed for clarity. Primary coordination spheres of Fe ions in **1-Xyl, 2-iPr, 3-iPr** and **3-tBu** respectively, with pertinent bond lengths in Å (bottom). H, C, N and Fe atoms are shown as green, grey, dark blue and orange ellipsoids, respectively. The t-butyl group and one ethyl moiety in **3-tBu,** and one of the ethyl substituents and the one of the phenyl rings in **3-iPr** were positionally disordered; the depicted structures represent the models with ≥50% occupancy for the disordered fragment.

geometric constraints afforded by the cyclophane ligand used here.[16] The mononuclear complex can also accommodate a third isocyanide donor to form a tris(isocyanide) Fe(I) complex, which is similar to the related polycarbonyl Fe(I) β-diketiminate complexes.[58] By contrast, NMR spectra of **1-Xyl** were unchanged upon the addition of excess XylNC, even with heating to 60°C for 24 h. [59] Together with prior observations for CO and N_2 coordination to diiron complexes of this ligand, we conclude that the $\mathbf{L}^{2-}$ ligand effectively controls the coordination number and the local coordination geometry of each metal center within the complex.

We then reacted $Fe_2(\mu\text{-H})_2\mathbf{L}$ with 2 equiv. of isopropyl isocyanide (iPrNC), which yielded a C_s symmetric product **2-iPr** lacking the IR-absorptions in the 1700–2200 cm^{-1} range (Figure S6, S8). In the solid-state structure of **2-iPr**, insertion of an iPrNC into each μ-hydride affords the bis[μ-κ*C*:κ*N*-(isopropyl)iminoformyl]diiron complex (Figure 1). Longer C–N bond lengths of 1.2908(1) Å and 1.2944(1) Å and more acute C–N–C_{iPr} bond angles (121.90(1)° and 122.45(1)°) compared to those in **1-Xyl** support decreased CN bond order.[60–62] The nominally coplanar β-diketiminate arms in **2-iPr** with a dihedral angle between BDI planes of 172.951(1)° as compared to **1-Xyl** and to other complexes of $\mathbf{L}^{2-}$ reveals the flexibility of this cyclophane ligand to accommodate the steric demands of the iPr group.[24,63]

Formation of **2-iPr** is expected to be stepwise, traversing a (μ-hydrido)(μ-iminoformyl) complex. Then, reaction of $Fe_2(\mu\text{-H})_2\mathbf{L}$ with 1 equiv. of *i*PrNC expectedly generated the (μ-hydrido)(μ-κ*C*:κ*N*-iminoformyl) diiron(II) complex, **3-iPr**, based on ^{1}H-NMR, IR, and single crystal X-ray diffraction (XRD) data (Figure 1, S9, S11). From XRD data on single crystals of **3-iPr**, the μ-1,2-iminoformyl bridges the Fe centers outside of the cyclophane arene cavity, consistent with the greater steric accessibility of this hydride as compared to the hydride within the ligand cavity (Figure 1). Addition of a second equiv. of *i*PrNC to **3-iPr** yielded **2-iPr**,

corroborating the stepwise formation of **2-iPr** from $Fe_2(\mu\text{-H})_2$**L** (Figure S12). Ligand flexibility is again evident with substantial pinching of the cyclophane cavity—the arene-arene dihedral angle is 19.752(2)°— attributed to the relative differences in steric demands of hydride vs. the (isopropyl)iminoformyl (Figure S24).

To probe steric effects of the isocyanide substituent on the reaction, $Fe_2(\mu\text{-H})_2$**L** was treated reacted with methyl- or phenyl isocyanide, which yielded product mixtures with ^{1}H-NMR and IR spectra consistent with migratory insertion products (Figure S16-S18, S20-S23). The crystal structure for the product of the reaction with 1 equiv. methyl isocyanide (MeNC), **3-Me**, evidences insertion of MeNC into the *less* accessible hydride within the cyclophane cavity, implying that the internal hydride is more reactive (Figure. S19). Selective formation of **3-iPr** and **3-tBu** (*vide infra*) in which the isocyanide insertion is at the more accessible hydride indicates that the site of reaction is finely balanced between substrate and ligand steric effects and electronic factors. Insertion reactivity for PhNC as for the alkyl isocyanides implies that the steric consequences of the two *ortho*-methyl groups in XylNC precludes migratory insertion and leads to reductive elimination instead. Steric clashes from the two *ortho*-methyl groups in the xylyl group and the iminoformyl (if formed) would orient the iminoformyl out-of-plane with the xylyl ring, introducing steric conflicts between the ligand arene or Et groups.[64–71]

Similarly, reaction of $Fe_2(\mu\text{-H})_2$**L** with 1 equiv. of *tert*-butyl isocyanide (tBuNC) at ambient temperature afforded **3-tBu**, the *tert*-butyl analog of **3-iPr**, with comparable ^{1}H-NMR, IR, and XRD data (Figure 1, S13, S15). In contrast to the reaction of $Fe_2(\mu\text{-H})_2$**L** with iPrNC, reaction of either $Fe_2(\mu\text{-H})_2$**L** with more than 2 equiv. *t*BuNC or of **3-tBu** with additional equiv. of *t*BuNC results only in **3-tBu**, even with heating to 60 °C for 1 d. We conclude then that, the steric demands of the tBu- group preclude migratory insertion of a second equiv. of tBuNC. A similar outcome

was recently reported by Crimmin and coworkers for a tetrameric magnesium hydride cluster for which reaction with XylNC results in insertion into two of the Mg–(μ-H) bonds whereas MeNC inserted into all four hydride sites.[72] The XRD structure of **3-tBu** is isostructural with that of **3-iPr**, with comparable positions of the bridging iminoformyl outside of the cyclophane cavity (Figure 1) Electron density corresponding to the bridging hydride was evident in and could be readily modeled from the XRD data of **3-tBu**. The dihedral angle between the BDI arms in **3-tBu** and that in **3-iPr** (*viz.* 147.218(1)° and 131.972(3)°, respectively), suggest that the steric demands of the *tert*-butyl group in **3-tBu** are relieved by an outward rotation of the BDI arms.

The steric effects observed can arise from an initial associative step followed by either reductive elimination or migratory insertion. Therefore, we qualitatively evaluated the differences in overall reaction rate as a function of substituent. Assuming that the form of the rate laws for migratory insertion are substrate independent, we reacted solutions of $Fe_2(\mu\text{-H})_2$**L (**20.61 mM) and methyl-, isopropyl-, and t-butyl isocyanides (43.30 mM), and recorded NMR spectra at different time points at ambient temperature after mixing. In all cases, the first insertion was complete prior to the first recorded measurement at ~10 min after mixing, with complete consumption of $Fe_2(\mu\text{-H})_2$**L** (Figure S27-S29). However, a rate difference was observed for the second insertion with **2-iPr** requiring ~48 min to completely convert to **3-iPr** whereas the double insertion reaction with MeNC was complete within 15 min (Figure S20-S21 and S28-S29).

The retained hydrides in complexes **3** are presumed competent for migratory insertion given the conversion of **3-iPr** to **2-iPr**. However, we were keen to explore reaction with substrates for which insertion is unlikely. Treating **3-tBu** with XylNC at ambient temperature in a J-Young NMR tube with C_6D_6 as the solvent, surprisingly yielded **1-Xyl** as the only observable paramagnetic product by ^{1}H-NMR spectroscopy (Figure S30). To explore the fate of the iminoformyl ligand, we recorded

^{1}H NMR and mass spectra of the volatile species in this product mixture (Figure S31, S32). Of the chemical shifts observed in the volatile species NMR spectrum, the resonances at δ = 1.14 and 3.79 ppm are consistent with 1,3,5-tri-*tert*-butylhexahydro-1,3,5-triazine, which is one reported product of oligomerization of *tert*-butylaldimine.[73] ESI-HRMS(+) of the volatile products showed an ion envelope at *m*/*z* = 86.0969, as expected for *tert*-butylaldimine, tBuNCH$_2$ (Figure. S31). The aldimine likely forms by the reductive elimination of iminoformyl and hydride ligands in **3-tBu** although such a transformation remains rare given the propensity of isocyanides to readily insert into metal-hydrogen and metal-carbon bonds.[17] However, the presence of other as yet unidentified volatile organic products suggests other pathways are possible for the reaction of **3-tBu** with an isocyanide incapable of inserting into the Fe-(μ-H)-Fe bond.

Aware that detailed kinetic studies are needed to support an associative or dissociative mechanism for the reaction of isocyanides with between Fe$_2$(μ-H)$_2$**L**, the coordinatively unsaturated metal centers in Fe$_2$(μ-H)$_2$**L** hint at an associative mechanism (Scheme 3). We cannot exclude an equilibrium between Fe$_2$(μ-H)$_2$**L** and a Kubas complex, although work on a related system suggests such a Kubas complex must bind H$_2$ strongly or exhibit facile oxidative addition.[74] H$_2$ elimination is not also observed from Fe$_2$(μ-H)$_2$**L** upon heating or UV irradiation (280 nm or 360 nm), suggesting reductive elimination is disfavored in the absence of substrate.[75] Prior reactivity studies by our group on the related tri(μ-hydrido)triiron(II) cluster supported on a tris(β-diketiminate) cyclophane suggested that bridging hydrides can readily change coordination modes from μ^2 to semi-bridging, μ^3 or terminal.[74,76,77] Taken together, we propose an associative pathway wherein isocyanide coordination leads to isomerization of the hydride coordination modes (A to B). Binuclear reductive elimination is symmetry forbidden implying that isomerization is necessary to generate a terminal hydride competent for elimination.[78] We speculate that the

transient species observed in NMR spectroscopy could be one of the structures corresponding to intermediates A, B, or C, with the identity being dependent on the rates of isomerization, reductive elimination, and strength of the Fe–H_2 interaction. Prior work by Hong, et al, on the related trinucleating cyclophane suggest that isomerization should be facile and the structure of B is reminiscent of the N_2 bridged complex reported by Torres, et al, supporting Intermediate B as a preferred assignment.[63] Where insertion is preferred over reductive elimination, migratory

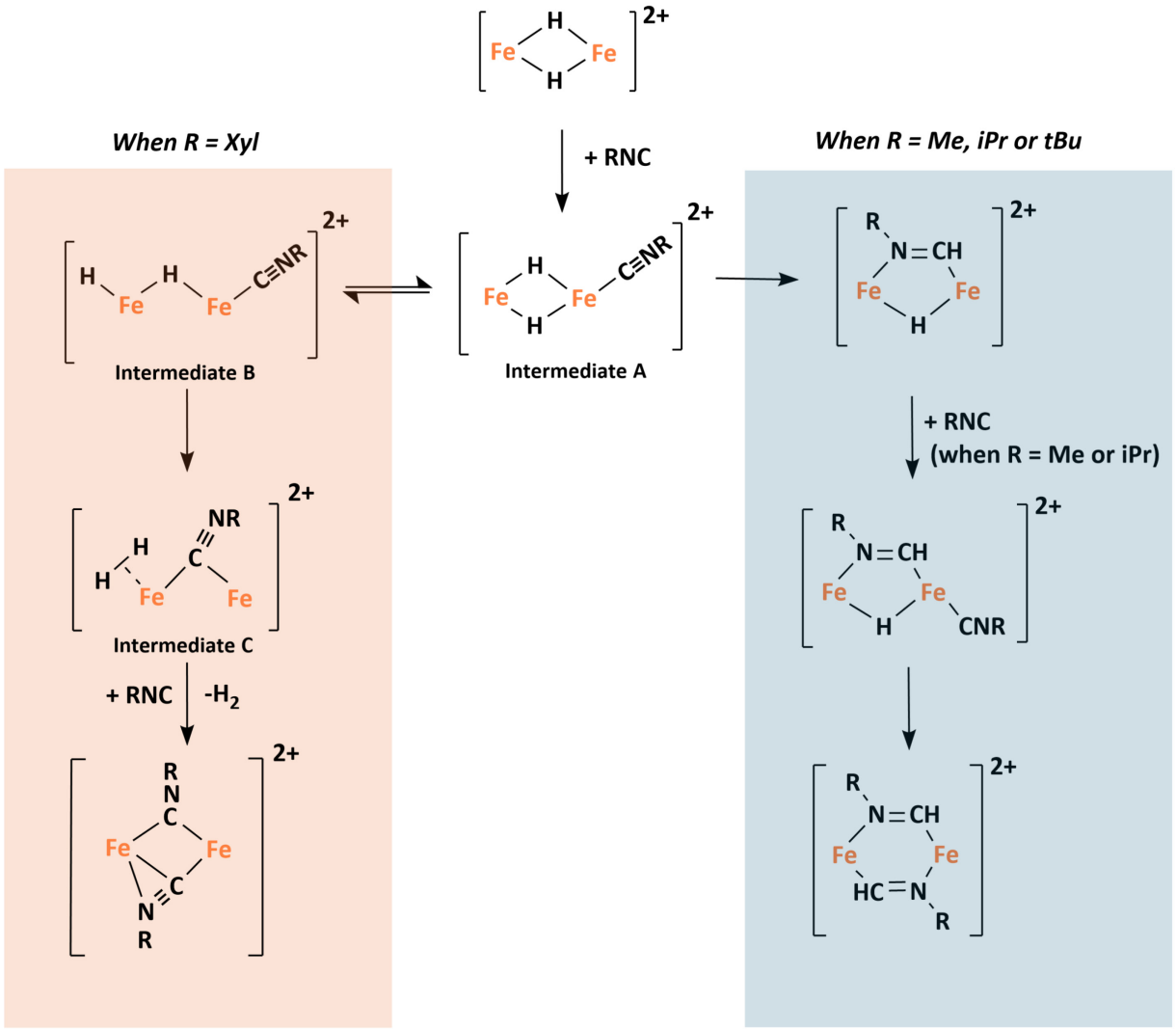

Scheme 3. Proposed reaction mechanism for the reaction of the isocyanides with $Fe_2(\mu\text{-}H)_2$**L**.

insertion may occur from intermediate A to directly access the iminoformyl product. An analogous second insertion, if sterically accessible, then affords the bis(iminoformyl) complexes.

Our observations here of xylyl isocyanide resulting in H_2 elimination whereas other isocyanides undergoing migratory insertion to the iminoformyl contrasts with Riera and coworkers' report (Scheme 1).[22] In that report, the steric demands of the ancillary ligand (*i.e.* phosphine donor) control reductive elimination versus migratory insertion, with a more sterically encumbered ancillary ligand yields insertion products whereas a less encumbering ligand affords reductive elimination products.[22] Similar to our observations of substrate steric effects dictating reaction outcome, Alt and coworkers' report that reaction of a di(hydrido)ditungsten complex with tBuNC effects H_2 reductive elimination whereas treatment with MeNC gives a 1,2-insertion product (Scheme 1).[23] The discrimination for elimination observed here, however, is reserved only to xylyl isocyanide, and may arise from the unique steric conflicts imposed by the two *ortho*-methyl groups, whereas steric bulk of the isonitrile substituent correlates with whether one or both hydrides are competent for insertion.[79]

The semi-hydrogenation of tBuNC to $tBuNCH_2$ by a diiron dihydride cluster is reminiscent of the MeNC reduction products produced by the nitrogenase cofactors.[10] Contrastingly, the proposed reaction pathway for the nitrogenase cofactor traverses an aminocarbene transient vs. the iminoformyl observed here. To our knowledge, aldimine reductive eliminations are exceedingly rare and only observed for late 3*d* metal hydrides. The prior report from Figueroa and coworkers results from the steric crowding at the metal center because of the sterically demanding terphenyl isocyanides.[12] Ligand steric conflicts here are manifested by cavity shape and size, with the former limiting the rotation of the xylyl group needed for migratory insertion and the latter controlling the extent of insertion (*i.e.*, one vs. two hydrides). With respect to aldimine elimination then,

coordination of the π-acidic xylyl isocyanide electronically primes the metal centers for reductive elimination, likely proceeding by a mechanism involving cluster core reorganization similar to the proposed isomerization of Intermediate A to Intermediate B. Similar structural changes to local environment of the iron centers have been previously noted in dinitrogen and CO coordination to related complexes.[24,63,76]

Conclusions

In conclusion, the reactivity of a low-coordinate di(μ-hydrido)diiron(II) complex, $Fe_2(\mu\text{-}H)_2$**L**, with various isocyanides leads to reductive elimination of H_2 for XylNC or to migratory insertion for all other isocyanides tested. Migratory insertion can be arrested by either control of reaction equivalents or by the steric demands of the isocyanide substituent. Analogous to the elimination of H_2 from $Fe_2(\mu\text{-}H)_2$**L** when treated with CO or XylNC, the reductive elimination of *tert*-butyl aldimine is also accessible with release of $tBuNCH_2$. The reactivity of these monohydride complexes as well as other transformations involving isocyanides are currently under investigation.

Accession Codes

CCDC 2353888-2353890, 2353893, and 2353894 contain the supplementary crystallographic data for this paper. These data can be obtained free of charge via www.ccdc.cam.ac.uk/data_request/cif, or by emailing data_request@ccdc.cam.ac.uk, or by contacting The Cambridge Crystallographic Data Centre, 12 Union Road, Cambridge CB2 1EZ, UK; fax: +44 1223 336033.

Associated content

The Supporting Information is available free of charge at https://pubs.acs.org/doi/10/1021.acs.inorgchem.XXXXXXX.

^{1}H NMR, IR, ESI(+)/HR-MS, and crystal data tables

AUTHOR INFORMATION

Corresponding Author

Leslie J. Murray– Center for Catalysis and Florida Center for Heterocyclic Chemistry, Department of Chemistry, University of Florida, Gainesville, FL 32611, U.S.A.

Author Contributions

The manuscript was written through contributions of all authors. All authors have given approval to the final version of the manuscript.

Funding Sources

T.S.J and L.J.M acknowledge funding from the National Science Foundation (CHE-2102098). X-ray diffractometers for measurements at the Center for X-Ray Crystallography at UF were supported by the National Science Foundation (CHE-1828064). Mass spectrometry data were collected on instrumentation supported by the National Institutes of Health (S10 OD021758-01A1 and S10 OD030250-01A1).

ACKNOWLEDGMENT

Authors acknowledge Dr. S. MacMillan for XRD data collection of **1-Xyl**, **2-iPr**, and **3-tBu**.

REFERENCES

(1) Rofer-DePoorter, C. K. A Comprehensive Mechanism for the Fischer-Tropsch Synthesis. *Chemical Reviews* **1981**, *81* (5), 447–474. DOI:10.1021/cr00045a002.

(2) Ertl, G. Primary Steps in Catalytic Synthesis of Ammonia. *Journal of Vacuum Science & Technology A: Vacuum, Surfaces, and Films* **1983**, *1* (2), 1247–1253. DOI:10.1116/1.572299.
(3) De Smit, E.; Weckhuysen, B. M. The Renaissance of Iron-Based Fischer-Tropsch Synthesis: On the Multifaceted Catalyst Deactivation Behaviour. *Chemical Society Reviews* **2008**, *37* (12), 2758–2781. DOI:10.1039/b805427d.
(4) Seefeldt, L. C.; Yang, Z.-Y.; Lukoyanov, D. A.; Harris, D. F.; Dean, D. R.; Raugei, S.; Hoffman, B. M. Reduction of Substrates by Nitrogenases. *Chemical Reviews* **2020**, *120* (12), 5082–5106. DOI:10.1021/acs.chemrev.9b00556.
(5) Hoffman, B. M.; Lukoyanov, D.; Yang, Z.-Y.; Dean, D. R.; Seefeldt, L. C. Mechanism of Nitrogen Fixation by Nitrogenase: The Next Stage. *Chemical Reviews* **2014**, *114* (8), 4041–4062. DOI:10.1021/cr400641x.
(6) Adamska, A.; Silakov, A.; Lambertz, C.; Rüdiger, O.; Happe, T.; Reijerse, E.; Lubitz, W. Identification and Characterization of the "Super-Reduced" State of the H-Cluster in [FeFe] Hydrogenase: A New Building Block for the Catalytic Cycle? *Angewandte Chemie - International Edition* **2012**, *51* (46), 11458–11462. DOI:10.1002/anie.201204800.
(7) Shima, T.; Zhuo, Q.; Hou, Z. Dinitrogen Activation and Transformation by Multimetallic Polyhydride Complexes. *Coordination Chemistry Reviews* **2022**, *472*, 214766. DOI:10.1016/j.ccr.2022.214766.
(8) Ballmann, J.; Munhá, R. F.; Fryzuk, M. D. The Hydride Route to the Preparation of Dinitrogen Complexes. *Chemical Communications* **2010**, *46* (7), 1013–1025. DOI:10.1039/B922853E.
(9) Carpenter, A. E.; Mokhtarzadeh, C. C.; Ripatti, D. S.; Havrylyuk, I.; Kamezawa, R.; Moore, C. E.; Rheingold, A. L.; Figueroa, J. S. Comparative Measure of the Electronic Influence of Highly Substituted Aryl Isocyanides. *Inorganic Chemistry* **2015**, *54* (6), 2936–2944. DOI:10.1021/ic5030845.
(10) Rubinson, J. F.; Corbin, J. L.; Burgess, B. K. Nitrogenase Reactivity: Methyl Isocyanide as Substrate and Inhibitor. *Biochemistry* **1983**, *22* (26), 6260–6268. DOI:10.1021/bi00295a034.
(11) Ionkin, A.; Solek, S.; Bryndza, H.; Koch, T. Isonitriles in Fischer-Tropsch Catalysis. *Catalysis Letters* **1999**, *61* (3–4), 139–141. DOI:10.1023/a:1019049628101.
(12) Carpenter, A. E.; Rheingold, A. L.; Figueroa, J. S. A Well-Defined Isocyano Analogue of HCo(CO)4. 1: Synthesis, Decomposition, and Catalytic 1,1-Hydrogenation of Isocyanides. *Organometallics* **2016**, *35* (14), 2309–2318. DOI:10.1021/acs.organomet.6b00297.
(13) Salsi, F.; Hagenbach, A.; S. Figueroa, J.; Abram, U. Na[Tc(CO)(CN p -F-Ar DArF2) 4]: An Isocyanide Analogue of the Elusive Na[Tc(CO) 5]. *Chemical Communications* **2023**, *59* (27), 4028–4031. DOI:10.1039/D3CC00946G.
(14) Agnew, D. W.; Moore, C. E.; Rheingold, A. L.; Figueroa, J. S. Kinetic Destabilization of Metal–Metal Single Bonds: Isolation of a Pentacoordinate Manganese(0) Monoradical. *Angewandte Chemie International Edition* **2015**, *54* (43), 12673–12677. DOI:10.1002/anie.201506498.
(15) Zhuo, Q.; Yang, J.; Zhou, X.; Shima, T.; Luo, Y.; Hou, Z. Dinitrogen Cleavage and Multicoupling with Isocyanides in a Dititanium Dihydride Framework. *J. Am. Chem. Soc.* **2024**, *146* (15), 10984–10992. DOI:10.1021/jacs.4c02905.
(16) Yu, Y.; Sadique, A. R.; Smith, J. M.; Dugan, T. R.; Cowley, R. E.; Brennessel, W. W.; Flaschenriem, C. J.; Bill, E.; Cundari, T. R.; Holland, P. L. The Reactivity Patterns of Low-

Coordinate Iron-Hydride Complexes. *Journal of the American Chemical Society* **2008**, *130* (20), 6624–6638. DOI:10.1021/JA710669W/SUPPL_FILE/JA710669W-FILE004.CIF.
(17) Boyarskiy, V. P.; Bokach, N. A.; Luzyanin, K. V.; Kukushkin, V. Y. Metal-Mediated and Metal-Catalyzed Reactions of Isocyanides. *Chemical Reviews* **2015**, *115* (7), 2698–2779. DOI:10.1021/cr500380d.
(18) Collet, J. W.; Roose, T. R.; Ruijter, E.; Maes, B. U. W.; Orru, R. V. A. Base Metal Catalyzed Isocyanide Insertions. *Angewandte Chemie - International Edition* **2020**, *59* (2), 540–558. DOI:10.1002/anie.201905838.
(19) Beringhelli, T.; D'Alfonso, G.; Minoja, A.; Ciani, G.; Moret, M.; Sironi, A. Insertion of Isocyanides into Metal-Hydrogen Bonds in Triangular Hydrido-Carbonyl Clusters of Rhenium. X-Ray Crystal Structures of [Re3(μ-H)3(μ-H2-CHNR)(CO)10]− (R = p-Tolyl) and of [Re3(μ-H)3(M3-H2-CHNR)(CO)9]− (R = Cyclohexyl). *Organometallics* **1991**, *10* (9), 3131–3138. DOI:10.1021/om00055a029.
(20) Alvarez, M. A.; García, M. E.; García-Vivó, D.; Ruiz, M. A.; Vega, M. F. Insertion, Rearrangement, and Coupling Processes in the Reactions of the Unsaturated Hydride Complex [W2(H5-C5H 5)2(H)(μ-PCy2)(CO)2] with Isocyanides. *Organometallics* **2013**, *32* (16), 4543–4555. DOI:10.1021/om400439d.
(21) Anslyn, E. V.; Green, M.; Nicola, G.; Rosenberg, E. Mechanistic Studies on Metal to Ligand Hydrogen Transfer in the Thermal Reactions of H(μ-H)Os3(CO)10(CNR): Evidence for Proton Barrier Tunneling in a Metal to Ligand Hydrogen Transfer. *Organometallics* **1991**, *10* (8), 2600–2605. DOI:10.1021/om00054a019.
(22) Alonso, F. J. G.; Sanz, M. G.; Riera, V.; Abril, A. A.; Tiripicchio, A.; Ugozzoli, F. Reactions of Unsaturated Dihydrido Carbonyl Complexes of Manganese(I) with Nitriles and Isonitriles. Preparation and Characterization of the First Binuclear μ,H1,H2-NCR Derivatives. *Organometallics* **1992**, *11* (2), 801–808. DOI:10.1021/om00038a045.
(23) Alt, H. G.; Frister, T. Darstellung Eines Dimetallacyclopropen-Komplexes Durch Insertion von Methylisonitril in Eine W□H□W-Brücke. *Journal of Organometallic Chemistry* **1985**, *293* (1), C7–C9. DOI:10.1016/0022-328X(85)80255-2.
(24) Singh, D.; Knight, B. J.; Catalano, V. J.; García-Serres, R.; Maurel, V.; Mouesca, J.-M.; Murray, L. J. Partial Deoxygenative CO Homocoupling by a Diiron Complex. *Angewandte Chemie International Edition* **2023**, *62* (41), e202308813. DOI:10.1002/anie.202308813.
(25) Schuster, R. E.; Scott, J. E.; Casanova Jr., J. Methyl Isocyanide. *Organic Syntheses* **2003**, 75–75. DOI:10.1002/0471264180.os046.23.
(26) *CrysAlisPro; Rigaku OD, The Woodlands, TX, 2015.*
(27) Sheldrick, G. M. A Short History of SHELX. *Acta Cryst A* **2008**, *64* (1), 112–122. DOI:10.1107/S0108767307043930.
(28) Sheldrick, G. M. SHELXT – Integrated Space-Group and Crystal-Structure Determination. *Acta Cryst A* **2015**, *71* (1), 3–8. DOI:10.1107/S2053273314026370.
(29) Müller, P. Practical Suggestions for Better Crystal Structures. *Crystallography Reviews* **2009**, *15* (1), 57–83. DOI:10.1080/08893110802547240.
(30) Bruker Nano, Inc. APEX3 V2019, 2019.
(31) Bruker Nano, Inc. SAINT V8.40A, 2019.
(32) Bruker Nano, Inc. SADABS V2016/2, 2019.
(33) Sheldrick, G. M. Crystal Structure Refinement with SHELXL. *Acta Cryst C* **2015**, *71* (1), 3–8. DOI:10.1107/S2053229614024218.

(34) Singleton, E.; Oosthuizen, H. E. Metal Isocyanide Complexes. *Advances in Organometallic Chemistry* **1983**, *22*, 209–310. DOI:10.1016/S0065-3055(08)60404-9.
(35) Chisholm, M. H.; Cotton, F. A.; Extine, M. W.; Rankel, L. A. Reactions of Metal-to-Metal Multiple Bonds. 2. Reactions of Bis(Cyclopentadienyl)Tetracarbonyldimolybdenum with Small Unsaturated Molecules. Structural Characterization of .Mu.-Dimethylaminocyanamide-Bis(Cyclopentadienyl)Tetracarbonyldimolybdenum. *Journal of the American Chemical Society* **1978**, *100* (3), 807–811. DOI:10.1021/ja00471a025.
(36) Gade, L. H.; Schubart, M.; Findeis, B.; Fabre, S.; Bezougli, I.; Lutz, M.; Scowen, I. J.; McPartlin, M. Synthesis and Reactivity of Early−Late Heterodinuclear Complexes Stabilized by a Trisilylsilane-Based Tripodal Amido Ligand. *Inorganic Chemistry* **1999**, *38* (23), 5282–5294. DOI:10.1021/ic990562n.
(37) Friedrich, S.; Gade, L. H.; Scowen, I. J.; McPartlin, M. A Chelate-Amidozirconium Fragment as Building Block for Unsupported Trinuclear ZrM2 Heterobimetallic Complexes (M = Fe, Ru, Co). *Angewandte Chemie International Edition in English* **1996**, *35* (12), 1338–1341. DOI:10.1002/anie.199613381.
(38) Ohki, Y.; Araki, Y.; Tada, M.; Sakai, Y. Synthesis and Characterization of Bioinspired [Mo2Fe2]–Hydride Cluster Complexes and Their Application in the Catalytic Silylation of N2. *Chemistry – A European Journal* **2017**, *23* (53), 13240–13248. DOI:10.1002/chem.201702925.
(39) Bernal, I.; Brunner, H.; Wachter, J. Crystal and Molecular Structure of Triclinic [C5H5(CO)2Mol2(μ,H2-C□NC6H5) and Comparison with Its Monoclinic Form. *Journal of Organometallic Chemistry* **1984**, *277* (3), 395–401. DOI:10.1016/0022-328X(84)80724-X.
(40) Brunner, H.; Buchner, H.; Wachter, J.; Bernal, I.; Ries, W. H. Reactivity of the Metal□metal-Multiple Bond in Metal Carbonyl Derivatives: VI. Investigation into the Reaction of [C5Me5(CO)2Mo]2 with CH3N□C□S: Formation and Crystal Structure of (C5Me5)2(CO)4Mo2(μ,H2-C□NCH3). *Journal of Organometallic Chemistry* **1983**, *244* (3), 247–255. DOI:10.1016/S0022-328X(00)98616-9.
(41) Li, Q.; Luo, C.; Song, L. Reactions of Cyclohexyl Isocyanide with H5-Substituted Cyclo-Pentadienyl Mo□Mo Triply Bonded Complexes. Crystal Structure of [Mo(CO)2(H5-C5H4CO2CH3)]2(μ-H2-CNC6H11). *Chinese Journal of Chemistry* **2009**, *27* (9), 1711–1715. DOI:10.1002/cjoc.200990288.
(42) Bernal, I.; Draux, M.; Brunner, H.; Hoffmann, B.; Wachter, J. Reaction of (C5H5)2Mo2(CO)4 with Carbodiimides: Structural Characterization of C5H5(CO)2Mo(CNPh)Mo(NPh)C5H5, a Novel Complex Containing a Terminal Phenylimido and a Bridging Phenyl Isocyanide Ligand, and Its Reaction with P(OMe)31. *Organometallics* **1986**, *5* (2), 100229–100273.
(43) Adams, H.; Bailey, N. A.; Bannister, C.; Faers, M. A.; Fedorko, P.; Osborn, V. A.; Winter, M. J. The Addition of Isonitriles to [{M(CO)2(η-C5H5)}2] (M = Mo or W). Syntheses and Properties of [M2(μ-H2-CNR)(CO)4(η-C 5H5)2] (M = Mo or W, R = Me or But) and [{Mo(CNR)(CO)2(η-C5H5)}2] (R = Me or But)... *Journal of the Chemical Society, Dalton Transactions* **1987**, No. 2, 341–348. DOI:10.1039/DT9870000341.
(44) Herrmann, W. A.; Menjon, B.; Herdtweck, E. Chemistry of Oxophilic Transition Metals. 4. Reactivity of the Organozirconium(III) Complex (.Mu.-.Eta.5:.Eta.5-C10H8)[(.Mu.-Cl)Zr(.Eta.5-C5H5)]2 with Diphenyldiazomethane, Tert-Butyl Isocyanide, and Trimethylsilyl Azide: Diazo, Cyano, and Imido Complexes. *Organometallics* **1991**, *10* (7), 2134–2141. DOI:10.1021/om00053a015.

(45) Alvarez, M. A.; Amor, I.; García, M. E.; García-Vivó, D.; Ruiz, M. A.; Sáez, D.; Hamidov, H.; Jeffery, J. C. Activity of Mo–Mo and Mo–P Multiple Bonds at the Phosphinidene Complex [Mo2Cp2{μ-P(2,4,6-C6H2tBu3)}(μ-CO)2] in Reactions with Isocyanides and Phosphine Ligands. *Inorganica Chimica Acta* **2015**, *424*, 103–115. DOI:10.1016/j.ica.2014.04.043.

(46) Cuenca, T.; Gomez, R.; Gomez-Sal, P.; Rodriguez, G. M.; Royo, P. Reactions of Titanium- and Zirconium(III) Complexes with Unsaturated Organic Systems. X-Ray Structure of {[(.Eta.5-C5H5)Zr(CH3)]2[.Mu.-.Eta.1-.Eta.2-CN(Me2C6H3)] (.Mu.-.Eta.5-.Eta.5-C10H8)}. *Organometallics* **1992**, *11* (3), 1229–1234. DOI:10.1021/om00039a032.

(47) Li, B.; Xu, S.; Song, H.; Wang, B. Reactions of (Me2C)(Me2Si)[(H5-C5H3)Mo(CO)3]2 with Nitrile and Subsequent Cleavage of the CN Bond by Cooperation of Molybdenum and Ruthenium. *Journal of Organometallic Chemistry* **2008**, *693* (1), 87–96. DOI:10.1016/j.jorganchem.2007.10.026.

(48) Riera, V.; Ruiz, M. A.; Villafañe, F.; Bois, C.; Jeannin, Y. Synthesis, Crystal Structure and Heterometallic Derivatives of [Mo2Cp2(μ-σ,π-CNtBu)(PPh2CH2PPh2-P)(CO)3] (tBu = C(CH3)3, Cp = η-C5H5). *Journal of Organometallic Chemistry* **1990**, *382* (3), 407–417. DOI:10.1016/0022-328X(90)80218-O.

(49) Caselli, A.; Solari, E.; Scopelliti, R.; Floriani, C. A Synthetic Methodology to Niobium Alkylidenes: Reactivity of a NbNb Double Bond Anchored to a Calix[4]Arene Oxo Surface with Ketones, Aldehydes, Imines, and Isocyanides. *Journal of the American Chemical Society* **1999**, *121* (36), 8296–8305. DOI:10.1021/ja990647n.

(50) Yeo, A.; Shaver, M. P.; Fryzuk, M. D. A New Side-on End-On Ditantalum Dinitrogen Complex and Its Reaction with BuSiH3. *Zeitschrift für anorganische und allgemeine Chemie* **2015**, *641* (1), 123–127. DOI:10.1002/zaac.201400167.

(51) Fryzuk, M. D.; Johnson, S. A.; Rettig, S. J. New Mode of Coordination for the Dinitrogen Ligand: A Dinuclear Tantalum Complex with a Bridging N2 Unit That Is Both Side-On and End-On. *Journal of the American Chemical Society* **1998**, *120* (42), 11024–11025. DOI:10.1021/ja982377z.

(52) Pun, D.; Lobkovsky, E.; Chirik, P. J. Indenyl Zirconium Dinitrogen Chemistry: N2 Coordination to an Isolated Zirconium Sandwich and Synthesis of Side-on, End-on Dinitrogen Compounds. *Journal of the American Chemical Society* **2008**, *130* (18), 6047–6054. DOI:10.1021/ja801021w.

(53) Fryzuk, M. D.; Johnson, S. A.; Patrick, B. O.; Albinati, A.; Mason, S. A.; Koetzle, T. F. New Mode of Coordination for the Dinitrogen Ligand: Formation, Bonding, and Reactivity of a Tantalum Complex with a Bridging N2 Unit That Is Both Side-On and End-On. *Journal of the American Chemical Society* **2001**, *123* (17), 3960–3973. DOI:10.1021/ja0041371.

(54) Wang, B.; Luo, G.; Nishiura, M.; Hu, S.; Shima, T.; Luo, Y.; Hou, Z. Dinitrogen Activation by Dihydrogen and a PNP-Ligated Titanium Complex. *Journal of the American Chemical Society* **2017**, *139* (5), 1818–1821. DOI:10.1021/jacs.6b13323.

(55) Mo, Z.; Shima, T.; Hou, Z. Synthesis and Diverse Transformations of a Dinitrogen Dititanium Hydride Complex Bearing Rigid Acridane-Based PNP-Pincer Ligands. *Angewandte Chemie International Edition* **2020**, *59* (22), 8635–8644. DOI:10.1002/anie.201916171.

(56) Kilpatrick, A. F. R.; Green, J. C.; Cloke, F. G. N. Reactivity of a Dititanium Bis(Pentalene) Complex toward Heteroallenes and Main-Group Element–Element Bonds. *Organometallics* **2017**, *36* (2), 352–362. DOI:10.1021/acs.organomet.6b00791.

(57) Benner, L. S.; Olmstead, M. M.; Balch, A. L. Structural Characterization of a Four-Electron Donating, Doubly-Bridging Isocyanide in (μ-*p*-CH3C6H4NC)Mn2(Ph2PCH2PPh2)2(CO)4. *Journal of Organometallic Chemistry* **1978**, *159* (3), 289–298. DOI:10.1016/S0022-328X(00)93806-3.
(58) Smith, J. M.; Sadique, A. R.; Cundari, T. R.; Rodgers, K. R.; Lukat-Rodgers, G.; Lachicotte, R. J.; Flaschenriem, C. J.; Vela, J.; Holland, P. L. Studies of Low-Coordinate Iron Dinitrogen Complexes. *J. Am. Chem. Soc.* **2006**, *128* (3), 756–769. DOI:10.1021/ja052707x.
(59) Cowley, R. E.; Golder, M. R.; Eckert, N. A.; Al-Afyouni, M. H.; Holland, P. L. Mechanism of Catalytic Nitrene Transfer Using Iron(I)-Isocyanide Complexes. *Organometallics* **2013**, *32* (19), 5289–5298. DOI:10.1021/OM400379P/SUPPL_FILE/OM400379P_SI_002.CIF.
(60) Adams, R. D.; Dawoodi, Z. Importance of Trinuclear Coordination in the Activation and Desulfurization of a Thioformamido Ligand by a Triosmium Cluster. *Journal of the American Chemical Society* **1981**, *103* (21), 6510–6512. DOI:10.1021/ja00411a048.
(61) Adams, R. D.; Dawoodi, Z.; Foust, D. F. Role of Heteroatoms in the Formation of Higher Nuclearity Transition-Metal Carbonyl Cluster Compounds. The Condensation of Small Clusters. *Organometallics* **1982**, *1* (2), 411–413. DOI:10.1021/om00062a036.
(62) Dieck, H. tom; Klaus, J.; Kopf, J. A Novel Type of Diazadiene Co-Ordination Behaviour. X-Ray Structure of a Rhodium Complex with Bridging Azomethine Groups. *Journal of the Chemical Society, Chemical Communications* **1982**, No. 11, 574–575. DOI:10.1039/C39820000574.
(63) Torres, J. F.; Oi, C. H.; Moseley, I. P.; El-Sakkout, N.; Knight, B. J.; Shearer, J.; García-Serres, R.; Zadrozny, J. M.; Murray, L. J.; Torres,] J F; Oi, C. H.; Knight, B. J.; Murray, L. J.; Moseley, I. P.; Zadrozny, J. M.; El-Sakkout, N.; García, R.; Shearer, J. Dinitrogen Coordination to a High-Spin Diiron(I/II) Species. *Angewandte Chemie International Edition* **2022**, *61* (22), e202202329–e202202329. DOI:10.1002/ANIE.202202329.
(64) Bhattacharya, S.; Saha, B. K. Inclusion of a Chiral Guest in a Centrosymmetric Organic Host Lattice. *CrystEngComm* **2011**, *13* (23), 6941–6944. DOI:10.1039/C1CE05600J.
(65) Blair, A. D.; Hendsbee, A. D.; Masuda, J. D. 1-(2,4,6-Triisopropyl-phen-yl)Ethanone. *Acta Crystallographica Section E: Structure Reports Online* **2011**, *67* (10), o2731–o2731. DOI:10.1107/S1600536811038293.
(66) Schowtka, B.; Müller, C.; Görls, H.; Westerhausen, M. Synthesis, Structures, and Spectroscopic Properties of 3-Aryl-5-(2-Pyridyl)Pyrazoles and Related Pyrazoles. *Zeitschrift für anorganische und allgemeine Chemie* **2014**, *640* (5), 916–925. DOI:10.1002/zaac.201300637.
(67) Ito, Y.; Takahashi, H.; Hasegawa, J.; Turro, N. J. Photocyclization of 2,4,6-Triethylbenzophenones in the Solid State. *Tetrahedron* **2009**, *65* (3), 677–689. DOI:10.1016/j.tet.2008.10.105.
(68) Takahashi, H.; Ito, Y. Low-Temperature-Induced Reversible Single-Crystal-to-Single-Crystal Phase Transition of 3,4-Dichloro-2′,4′,6′-Triethylbenzophenone. *CrystEngComm* **2010**, *12* (5), 1628–1634. DOI:10.1039/B922167K.
(69) Fukushima, S.; Ito, Y.; Hosomi, H.; Ohba, S. Structures and Photoreactivities of 2,4,6-Triisopropylbenzophenones. *Acta Crystallographica Section B: Structural Science* **1998**, *54* (6), 895–906. DOI:10.1107/S0108768198005515.
(70) Bąkowicz, J.; Skarżewski, J.; Turowska-Tyrk, I. Photo-Induced Structural Changes in Two Crystal Forms with Different Numbers of Independent Molecules. *CrystEngComm* **2011**, *13* (13), 4332–4338. DOI:10.1039/C0CE00795A.

(71) Chen, C.; Bellows, S. M.; Holland, P. L. Tuning Steric and Electronic Effects in Transition-Metal β-Diketiminate Complexes. *Dalton Trans.* **2015**, *44* (38), 16654–16670. DOI:10.1039/C5DT02215K.
(72) Yang, W.; White, A. J. P.; Crimmin, M. R. Cross-Coupling of CO and an Isocyanide Mediated by a Tetrameric Magnesium Hydride Cluster. *Chem. Sci.* **2024**, 10.1039.D4SC02638A. DOI:10.1039/D4SC02638A.
(73) Achternbosch, M.; Brieger, L.; Strohmann, C. Influence Of Lithium Coordinating Additives On The Structure Of Phenyldimethylsilyllithium. *Zeitschrift für anorganische und allgemeine Chemie* **2021**, *647* (9), 979–983.
(74) Anderton, K. J.; Knight, B. J.; Rheingold, A. L.; Abboud, K. A.; García-Serres, R.; Murray, L. J. Reactivity of Hydride Bridges in a High-Spin [Fe $_3$ (μ-H) $_3$] $^{3+}$ Cluster: Reversible H $_2$ /CO Exchange and Fe–H/B–F Bond Metathesis. *Chem. Sci.* **2017**, *8* (5), 4123–4129. DOI:10.1039/C6SC05583D.
(75) Kubas, G. J. Fundamentals of H2 Binding and Reactivity on Transition Metals Underlying Hydrogenase Function and H2 Production and Storage. *Chem. Rev.* **2007**, *107* (10), 4152–4205. DOI:10.1021/cr050197j.
(76) Hong, D. H.; Ferreira, R. B.; Catalano, V. J.; García-Serres, R.; Shearer, J.; Murray, L. J. Access to Metal Centers and Fluxional Hydride Coordination Integral for CO2 Insertion into [Fe3(μ-H)3]3+ Clusters. *Inorganic Chemistry* **2021**, *60* (10), 7228–7239. DOI:10.1021/ACS.INORGCHEM.1C00244.
(77) Hong, D. H.; Murray, L. J. Carbon Dioxide Insertion into Bridging Iron Hydrides: Kinetic and Mechanistic Studies. *European Journal of Inorganic Chemistry* **2019**, *2019* (15), 2146–2153. DOI:10.1002/ejic.201801404.
(78) Trinquier, G.; Hoffmann, R. Dinuclear Reductive Eliminations. *Organometallics* **1984**, *3* (3), 370–380. DOI:10.1021/om00081a007.
(79) Pombeiro, A. J. L.; Guedes da Silva, M. F. C.; Michelin, R. A. Aminocarbyne Complexes Derived from Isocyanides Activated towards Electrophilic Addition. *Coordination Chemistry Reviews* **2001**, *218*, 43–74. DOI:10.1016/S0010-8545(01)00357-5.

SYNOPSIS

Here, we report the reactivity of isocyanides with a di(μ-hydrido)diiron(II) complex supported on a weak-field β-diketiminate ligand and observed that the reactivity was influenced by the identity of the substituent on the isocyanide. The results learned from this study can be used to understand the interaction of isocyanides and isoelectronic molecules (CO and N_2) with the catalysts with similar structural units.